Emergent Materials (2025) 8:6017–6037
https://doi.org/10.1007/s42247-025-01194-6

ORIGINAL ARTICLE

Viability of using 100% of recycled concrete aggregates for durable solid masonry blocks

Md Mohsin M Dafedar[1] · Balakrishna Rao K[1] · B. H. Venkataram Pai[1] · Gopal Bharamappa Bekkeri[1] · Kiran K. Shetty[1]

Received: 27 January 2025 / Accepted: 16 July 2025 / Published online: 25 August 2025
© The Author(s) 2025

Abstract
The generation of construction and demolition (C&D) waste is substantial and continues to grow annually. Despite this, only a limited portion of concrete byproducts have been repurposed using recycled concrete aggregates (RCAs) for concrete production. This study examines the feasibility of utilizing RCAs obtained from C&D waste in the production of solid masonry blocks (SMBs) for higher cement-to-aggregate (C:A) ratios. RCAs were used as replacements for natural coarse and fine aggregates in SMB manufacturing. The study assessed the influence of RCAs on the strength and durability properties of load-bearing SMBs. Results demonstrated a decline in strength and an increase in water absorption (WA) as the C:A ratio shifted from 1:6 to 1:24. Under exposure to sulfuric acid, strength losses ranged from 36.92% to 62.59%, while thermal conductivity values varied between 1.467 W/m°C and 0.371 W/m°C. Furthermore, when subjected to elevated temperatures of 200 °C to 800 °C, strength losses were observed to range from 1.87% to 65.80%. Nonetheless, SMBs with C:A ratios from 1:6 to 1:18 complied with the performance standards set by Indian guidelines. By incorporating RCAs, this research promotes sustainable construction practices, reducing the environmental impact of SMB production while enhancing their functional performance and durability.

Keywords Construction and demolition waste · Recycled concrete aggregates · Solid masonry blocks · Sustainable construction · Circular economy

1 Introduction

The rapid pace of urbanization has led to the generation of significant volumes of C&D waste, which is highly heterogeneous and comprises materials such as concrete, bricks, timber, metals, glass, plastics, gypsum, and excavated earth [1]. C&D waste constitutes a significant part of the solid waste sent to landfills, with daily waste including concrete debris, bricks, tiles, sand, dust, wood, metals, plastic, and cardboard. In India, data from the Ministry of Housing and Urban Affairs in 2024 indicates that the country generates approximately 150 to 500 million tonnes of C&D waste annually, contributing to about 35%–40% of the global C&D waste output. Despite this significant volume, a survey conducted by the Centre for Science and Environment reported that only about 1% of this waste was being recycled. This low recycling rate has led to serious environmental and social concerns, especially as the continued reliance on concrete in the construction sector intensifies the depletion of natural aggregates (NAs), thereby worsening issues related to resource scarcity [2]. Currently, the predominant method for managing C&D waste is landfilling, which often leads to secondary environmental pollution. To address this issue, the development of low-carbon building materials using C&D waste has gained significant attention as a sustainable strategy for their reuse and recycling. This shift reflects a broader movement toward environmentally conscious construction practices that aim to reduce carbon emissions and preserve natural resources. Although a large portion of recycled C&D waste is typically downcycled for use in lower-value applications such as road sub-base layers, engineering fill, or landfill cover, its use in high-value

✉ Kiran K. Shetty
kiran.shetty@manipal.edu

[1] Department of Civil Engineering, Manipal Institute of Technology, Manipal Academy of Higher Education, Manipal 576104, Karnataka, India

applications, particularly as a substitute for NAs in concrete, remains limited.

Utilizing C&D waste to produce recycled aggregates for concrete is a highly effective approach to managing solid waste, offering two key advantages: conserving natural resources and minimizing land use. Based on particle size, crushed C&D waste can be classified into recycled powder (<0.15 mm), fine recycled concrete aggregate (FRCA) (0.15~5.00 mm), and coarse recycled concrete aggregate (CRCA) (5.00~31.5 mm) [3]. These materials have been successfully used as substitutes for NAs in mortar and concrete production. The development of recycled aggregate concrete (RAC), composed of both FRCA and CRCA, contributes to waste reduction, environmental protection, and the preservation of dwindling natural aggregate reserves, marking a significant step toward more sustainable construction practices [4]. This approach significantly reduces energy consumption and lowers emissions of CO_2, NO_x, and other pollutants associated with aggregate production. According to Hossain et al. [5], producing one tonne of natural aggregates such as river sand or crushed stone emits approximately 23–33 kg CO_2-eq, whereas producing one tonne of FRCAs from construction and demolition waste results in only about 12 kg CO_2-eq. Similarly, the production of natural coarse aggregates emits approximately 32 kg CO_2-eq per tonne, compared to just 11 kg CO_2-eq for CRCAs from C&D waste. This demonstrates that utilizing RCAs in place of NAs significantly lowers greenhouse gas emissions and mitigates other environmental impacts. Studies show that incorporating RCAs from C&D waste can provide considerable economic and environmental benefits, including a 10–20% reduction in material costs, up to a 65% decrease in greenhouse gas emissions, and a 58% reduction in non-renewable energy use [6].

In cement-based concrete, increasing the proportion of recycled aggregates often leads to reduced mechanical performance, with aggregate size playing a significant role; smaller recycled aggregates tend to result in lower concrete strength due to higher water absorption and the presence of adhered mortar [7]. The mechanical behaviour of RAC is particularly influenced by the quality and quantity of recycled aggregates, especially FRCAs under 4.75 mm. These finer particles typically contain more contaminants and weaker residual mortar, which can compromise the strength and durability of RAC [8]. Therefore, optimizing the production and utilization of FRCAs is critical to fully realizing the benefits of RAC in sustainable construction [9].

Environmental pollution and high energy usage are increasing concerns in the production of masonry units [10]. In India, burnt clay bricks have been a traditional masonry material for centuries, making the country the second-largest producer of these bricks worldwide after China [11]. Recent research on SMBs has focused on promoting low-carbon living and advancing green building practices, aiming to eliminate the use of clay and foster the development of eco-friendly SMBs. Significant studies have explored the effective use of RCAs in producing concrete bricks and blocks [12, 13]. Utilizing RCAs for mechanized moulded bricks and blocks presents numerous benefits compared to their use in structural concrete. These blocks and bricks are typically manufactured using automated moulding machines that shape concrete mixtures through vibration and compaction. This method makes the workability of the concrete, such as slump, less critical and requires less water for the mixes than RAC utilized for structural purposes. The resulting reduced water-to-cement (w/c) ratio enhances the strength of the concrete, while reduced water content minimizes creep and shrinkage in the hardened material [14].

Various researchers have explored the mechanical and durability properties of blocks and bricks incorporating recycled aggregates (RA). For instance, Poon et al. [15] developed moulded bricks and blocks using CRCAs of a 10 mm maximum size. Experimental tests were conducted to produce bricks measuring 225 × 105 × 75 mm, where natural coarse aggregates (NCAs) were substituted with RA (both coarse and fine) at varying levels from 25 to 100% in increments of 25%. The study assessed the compressive strength (CS), flexural strength (FS), drying shrinkage, and density of the bricks. Findings revealed that substituting up to 50% of NCAs with RA had no significant effect on the CS of the bricks. Nonetheless, at a full 100% replacement level, the CS decreased by 27%, from 16.2 MPa to 11.8 MPa. Despite this decrease, the RAC bricks complied with BS-6073 standards, meeting the minimum requirements for CS (>7 MPa) and FS (>0.65 MPa). Additionally, the bricks and blocks performed well in drying shrinkage and skid resistance evaluations.

Poon and Lam [16] carried out experimental investigations to evaluate the impact of different C:A ratios from 1:3 to 1:13 and aggregate types on the performance of concrete paving blocks. Their findings indicated that CS decreased with an increase in the C:A ratio and was closely associated with the crushing strength of the aggregates; higher-strength aggregates resulted in improved CS. WA of the blocks was also found to be directly influenced by the WA properties of the aggregates used. When using 100% RCA, the blocks did not meet the required WA limits unless the C:A ratio was reduced to 3. To produce high-quality, eco-friendly concrete blocks entirely from recycled materials, the study recommended using a 50:50 blend of recycled crushed glass and RCA, with a C:A ratio of 4 or lower. In further research, Poon et al. [17] analyzed the properties of concrete blocks produced using low-quality RA. They found that fine RA with higher soil content adversely affected the mechanical

properties of the blocks, with increased use of low-grade fine RA resulting in reduced strength and density. Nevertheless, the study suggested that low-quality RA from construction waste sorting facilities could be utilized for manufacturing non-structural precast concrete blocks.

Similarly, Guo et al. [18] developed masonry blocks using 75% RCAs and evaluated their durability and mechanical performance. Although RCAs have slightly decreased the CS and durability of the blocks, concrete blocks with 75% RCAs met Chinese standards for drying shrinkage, strength, and freeze–thaw resistance. The compressive and shear behaviour of masonry prisms made with RAC blocks and traditional mortar was similar to that of conventional masonry units. Moreover, RAC masonry blocks demonstrated a lower environmental impact than those made with natural aggregate concrete. Significant research has explored the viability of using RCAs in the manufacture of concrete bricks, with a concentration on enhancing their physical, mechanical, and durability characteristics while improving performance and sustainability in construction. Furthermore, substantial efforts have been dedicated to developing concrete products such as paving blocks for light traffic and curbs by partially or entirely substituting NCAs with RCAs, achieving promising results [19, 20]. For instance, Poon and Chan [21] demonstrated that the allowable contamination level of RCAs in paving block production could be increased from 1% to a maximum of 10%. These studies have shown that incorporating up to 100% CRCAs and FRCAs is feasible for producing non-structural concrete elements. However, achieving the required mechanical properties on average necessitates higher cement content in such precast applications.

Considering the novelty of the study, this research highlights the potential for a transformative approach in the construction industry through the adoption of SMBs, aligning with the United Nations'sustainability goals, particularly in a resource-rich country like India. The proposed use of RCAs not only reduces waste treatment costs and the consumption of virgin materials but also lowers CO_2 emissions, promoting environmentally friendly construction practices. By integrating RCAs, which are abundantly available as waste in India, into SMBs, the study opens avenues for cost-effective and sustainable building materials, particularly for affordable housing. The study highlights the critical role of adopting sustainable practices in construction by utilizing recycled materials, minimizing reliance on natural aggregates, and addressing waste management issues. The evaluation of RCA performance in masonry blocks provides valuable insights into their suitability for structural and non-structural applications, contributing to environmental preservation, resource efficiency, and cost-effective construction solutions with long-term durability benefits.

Despite this progress, limited research has focused on the development of load-bearing SMBs using a full replacement of NAs with RCAs obtained from C&D waste, combined with reduced cement content achieved through increased C:A ratios. This study aims to bridge this gap by designing load-bearing RCA-based SMBs, thereby promoting the large-scale recycling of C&D waste for sustainable construction practices. The research employs 100% CRCAs and FRCAs as replacements for NCAs and natural fine aggregates (NFAs), respectively. The study focused on analyzing the impact of various C:A ratios on the physical and mechanical properties of RCA-based SMBs and assessed their durability performance.

2 Materials and characterization

The study utilized ordinary Portland cement (OPC), CRCAs, FRCAs, and water as key ingredients for producing SMBs. Specifically, an OPC of 43 grade was used, adhering to IS 269:2015 [22] standards, with a specific gravity of 3.15 and fineness of 285 m^2/kg. Table 1 presents the chemical composition of the OPC and RCAs, determined through X-ray fluorescence (XRF) testing. The RCAs were sourced from the demolition of a 50-year-old building on the Kasturba Medical College campus in Manipal, Udupi district, Karnataka, India.

Concrete construction and demolition waste collected from the site was initially crushed using a jaw crusher, resulting in ungraded and unsorted aggregates. These were then mechanically sieved to separate them into CRCAs and FRCAs. FRCAs were identified as particles passing through a 4.75 mm sieve but retained on a 150-micron sieve. Compared to natural sand, FRCAs exhibited a more angular shape with some elongated and flat particles, along with a significantly rougher surface texture, whereas natural sand particles were generally rounded and smoother. Figure 1(a) shows the FRCA used in this study. The physical properties

Table 1 Chemical composition of the OPC and RCAs

Compounds	SiO_2	Al_2O_3	Fe_2O_3	CaO	MgO	K_2O	Na_2O	SO_3	LOI
OPC (%)	19.94	4.63	2.59	63.68	1.38	0.67	0.20	2.67	3.86
RCAs (%)	38.40	11.70	5.17	29.50	0.99	1.50	1.35	0.34	10.07

*LOI: – Loss of Ignition

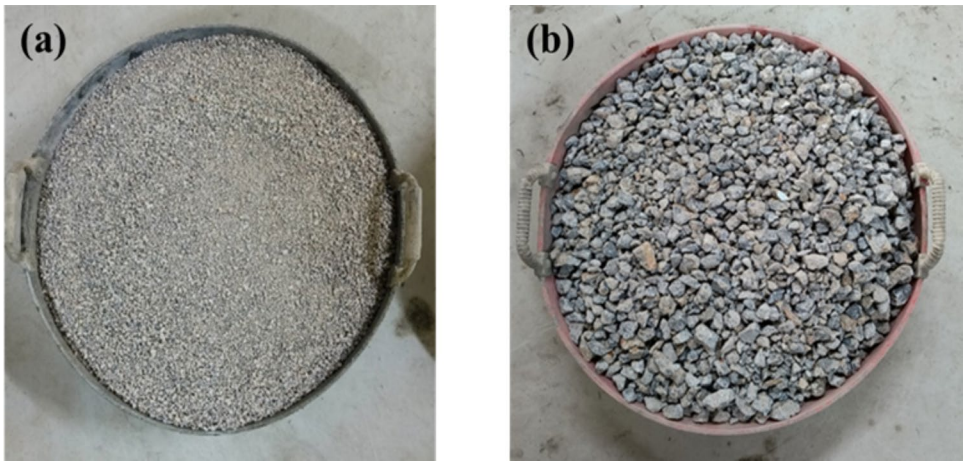


Fig. 1 (**a**) FRCA below 4.75 mm to 150-micron; (**b**) CRCA below 25 mm to 4.75 mm

Table 2 Physical and mechanical properties of RCAs

Properties	Referred to	CRCAs	FRCAs
Fineness modulus	IS-383 [23]	7.26	3.22
Bulk density (kg/m^3)	IS-2386 (III) [24]	1342.31	1335.83
Water absorption (%)	IS-2386 (III) [24]	3.95	6.96
Specific gravity	IS-2386 (III) [24]	2.5	2.47
Voids (%)	IS-2386 (III) [24]	46.29	45.92
Impact value (%)	IS-2386 (IV) [25]	34.3	-
Crushing value (%)	IS-2386 (IV) [25]	38.66	-
Abrasion value (%)	IS-2386 (IV) [25]	39.67	-
Flakiness and Elongation Index (%)	IS-2386 (I) [26]	22.89	-

of FRCAs were tested in accordance with IS 2386:1963 Part 3, and the results complied with the requirements of IS 383:2016, as presented in Table 2. CRCAs, which ranged in size from 25 mm to 4.75 mm, were similarly segregated as shown in Fig. 1(b) and underwent physical and mechanical testing following IS 2386:1963 Parts 1, 3, and 4, with results summarized in Table 2. These also met the IS 383:2016 specifications.

Furthermore, particle size distribution analyses for both aggregate types were conducted as per IS 383:2016 and were found to be within the permissible grading limits. The optimal proportions of 40% FRCA and 60% CRCA were determined based on the highest compaction test results. Additionally, these proportions align with those commonly used in low-grade concrete, as recommended by the Indian standard IS 456:2000 [27].

2.1 X-ray diffraction (XRD) of OPC and RCAs

The XRD patterns of RCAs and OPC are illustrated in Fig. 2. The OPC XRD pattern shows the presence of minerals such as alite (ICSD-4331 & 162744), belite (ICSD-182052), and calcium silicate (ICSD-963), which facilitate hydration upon exposure to water. The XRD analysis of RCA patterns primarily displays quartz peaks, with smaller peaks for calcite and anorthite. The relatively low intensity of calcite and anorthite peaks suggests their limited presence. Calcite could either form due to carbonation within the original concrete over time or result from the initial cement paste attached to the RCA surface [28]. The presence of quartz is likely linked to the mortar that remains on the surface of the aggregates. Similar XRD patterns for RCAs have been noted in research findings by M.C. Limbachiya et al. [29] and Baifa Zhang et al. [30].

3 Experimentation

3.1 Mix design

SMBs were produced using varying C:A ratios of 1:6, 1:8, 1:11, and 1:13, based on recommendations from different literature [31, 32]. Additional mix ratios were explored by progressively increasing the C:A ratios to 0.01:15, 1:18, 1:21, and 1:24 until the mixtures no longer met the strength requirements outlined in IS 2185 (Part 1) – 2005 [31]. These ratios aimed to create load-bearing SMBs. While the required strength for load-bearing structures varies between ASTM, British, and Indian standards, the Indian standard was chosen for this study due to its higher requirement threshold and wider application, targeting a CS of 5 MPa to identify the best combination. The parameters studied included the cement content and the proportion of RCAs in the C:A ratios. Eight concrete block mixes were developed, each containing different amounts of OPC and RCAs. These masonry blocks incorporated 100% RCA, consisting of both CRCAs and FRCAs. The mix details are presented in Table 3, showing the quantities required to produce one cubic meter of load-bearing SMBs. The different C:A ratios were expressed by their weights, where'C'represents OPC,'A'represents RCAs, and the numbers indicate the weight proportions. Based on the findings of the literature,

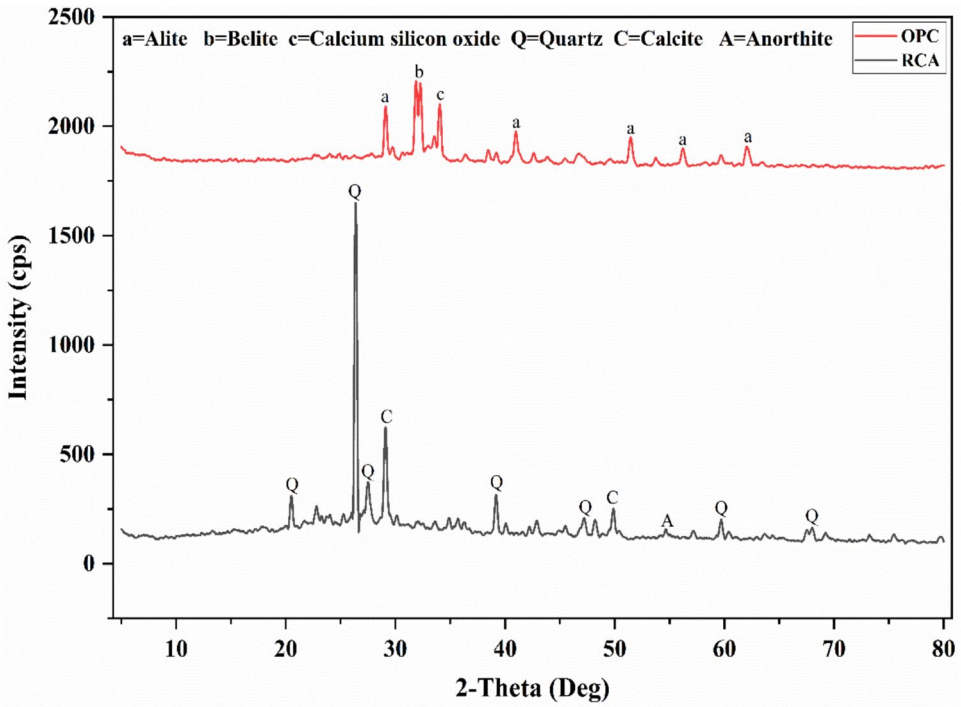


Fig. 2 XRD of OPC and RCAs

Table 3 Mix proportions

Mix ratio (C:A)	Water (kg/m^3)	OPC (kg/m^3)	FRCAs (kg/m^3)	CRCAs (kg/m^3)	w/c
1:6	153	306	725	1114	0.5
1:8	123	245	774	1189	0.5
1:11	94	189	819	1259	0.5
1:13	82	164	839	1290	0.5
1:15	72	145	855	1313	0.5
1:18	61	123	872	1340	0.5
1:21	53	107	885	1360	0.5
1:24	47	95	895	1375	0.5

the w/c ratio for all mixes was kept constant at 0.5 [10, 32], with slump values maintained between 0 and 10 mm.

3.2 Manufacturing of SMBs

The SMB samples were produced in the research lab using a dry-mix technique, as outlined in various studies [17, 32]. Initially, CRCAs and FRCAs were combined with OPC in a drum mixer and mixed for 3 to 5 min to achieve a uniform blend. Afterwards, a calculated amount of water was introduced, and the mixing process was carried on for another 4 to 8 min until a homogeneous, low-workability mix with a slump value between 0 and 10 mm was obtained. As we all know, RCAs demonstrate increased WA, which may decrease the overall properties of the concrete mix. Therefore, the aggregates were soaked in water for one hour before mixing. This one-hour soaking time was determined through multiple trials, with saturation intervals of 10 min, until the WA properties of the RCAs had minimal impact on the mix. In the dry-mix method, the pre-soaked water did not alter the w/c ratio, as the absorbed water by the RA contributed to cement hydration during the hardening phase [32]. The uniform mix was then poured into steel moulds measuring 300 mm × 200 mm × 200 mm, as specified by IS 2185 (Part 1) – 2005 [31]. The mixture was layered in three stages, and each layer was compacted by using the vibro compaction technique by placing the moulds on a vibrator table. After compaction, the moulds were left undisturbed for 24 h while wrapped with plastic sheets at the top to allow the initial strength to develop and stored under dry laboratory conditions where temperatures vary between 25 °C to 30 °C, as recommended by IS 456–2000 [27]. The curing process was performed at 90% humidity and a temperature of 27 ± 3 °C. After one day, the block specimens were demoulded and kept moist by covering them with wet gunny bags for 28 days to complete the curing process.

3.3 Tests conducted

3.3.1 Hardened density

The hardened density of the SMBs was evaluated following the method specified in IS 2185 (Part 1) – 2005 [31]. The blocks were first dried in a ventilated oven at 100 °C and then cooled to room temperature. Their dimensions were measured to calculate the net volume (Vnet) based on their length, width, and height. The blocks were subsequently weighed to obtain their dry mass (M_{dry}), following standard

protocols. The hardened density (ρ_b) was then determined using Eq. 1.

$$\rho_b = M_{dry}/V_{net} \quad (1)$$

3.3.2 Compressive strength

The CS of the SMBs was measured in accordance with the test procedures outlined in ASTM C90–09 [33]. These CS tests were performed 28 days after the blocks were produced. A testing device with a loading capacity of 3000 kN was utilized to measure the CS. The load was applied to the standard-sized masonry blocks of 300 mm × 200 mm at a constant rate of 5 kN/s. For each mix ratio, three specimens were tested, following the ASTM C90–09 guidelines [33].

3.3.3 Flexural strength

The FS of the SMBs was assessed following the procedure described by Dayaratnam, P −1987 [34], in accordance with IS 4860–1968 [35], after 28 days of curing. The experiment employed a three-point bending technique featuring a support span of 225 mm and a block height of 200 mm. It was conducted on a hydraulic universal testing apparatus that can support a maximum load of 300 kN. The load was applied progressively to the standard-sized masonry blocks of 300 mm × 200 mm at a rate of 10 kN/min. Three samples from every mix proportion were tested according to the relevant standards.

3.3.4 Water absorption

The WA properties of the SMBs were evaluated following IS 2185 (Part 1)—2005 [31]. After 28 days, the WA was determined by submerging oven-dried block samples in water at normal temperature for 24 h. The blocks were then removed and allowed to drain on a wire mesh for one minute. Any excess water from the surface was removed using a dry cloth, and the specimens were immediately weighed (Mwet). Following this, all specimens were dried in a vented oven at 100 °C to 115 °C for 24 h until two consecutive weighings, taken two hours apart, showed a moisture loss of no more than 0.2% of the previously recorded dry mass (M_{dry}). The WA percentage was calculated using Eq. 2 as the proportion of the absorbed water mass to the mass of the specimen after it had been oven-dried.

$$\text{Water absorption, in } \% = \frac{(\text{Mwet} - \text{Mdry})}{\text{Mdry}} \times 100 \quad (2)$$

3.3.5 Sorptivity

Sorptivity refers to a porous material's ability to take in and expel water via capillary action. This test was performed on oven-dried concrete test specimens for different ratios of blocks, which are 100 ± 6 mm diameter discs with a length of 50 ± 3 mm, in line with ASTM C1585- 04 [36]. The samples were initially stored within a desiccator inside an oven maintained at a temperature of around 50 ± 2 °C for 3 days, then partially submerged in water, with the level maintained approximately 1 to 3 mm above the base. The lateral water flow was prevented by sealing the surrounding surface using self-sticking plastic adhesive tape. The water absorbed at various intervals of time was measured, and the sorptivity, or rate of WA, was determined using Eqs. 3 and 4.

$$i = \frac{m_t}{(a \times d)} \quad (3)$$

$$i = S\sqrt{t} \quad (4)$$

3.3.6 Acid attack

At present, there are no standardized methods for evaluating SMBs under sulfuric acid attack. Nonetheless, the test was conducted in accordance with procedures described in the literature [37], with ASTM C1898-20 [38] providing general guidelines for assessing concrete's resistance to chemicals. To evaluate the acid resistance of SMBs with varying C:A ratios, the samples were submerged in a 5% sulfuric acid (H_2SO_4) solution for 90 days by weight of water under controlled laboratory conditions. Throughout this period, the pH of the masonry solid blocks was consistently monitored using both a pH meter and litmus paper to ensure it remained within the range of 2 and 3. Measurements were taken every 15 days and compared to the initial reference value. If any fluctuation in pH was observed during this interval, additional acid was introduced to the solution as needed to maintain the desired pH range of 2 and 3, as required. After being taken out from the solution, the samples were examined for loss of mass and strength using Eqs. 5 and 6.

$$Mass\ loss\ (\%) = \frac{M_1 - M_2}{M_1} \times 100 \quad (5)$$

wherein:

M_1 mass of masonry blocks after curing and before exposure to the attack (kg)

M_2 mass of masonry blocks after full exposure to the attack (kg)

$$Strength\ loss\ (\%) = \frac{f_{ck1} - f_{ck2}}{f_{ck1}} \times 100 \quad (6)$$

wherein:fck_1 CS of masonry blocks after curing and before being subjected to attack (MPa)
fck_2 CS of masonry blocks after being subjected to attack for 90 days (MPa)

3.3.7 Sulfate attack

Sulphates are commonly present in paints and plastering mortars, and their effects on masonry blocks can manifest as either internal or external sulphate attacks. External sulphate attack is typically simulated by immersing the specimens in a 5% sulfate solution. To assess the resistance of SMB specimens to sulphate attack, they were immersed in a solution comprising 5% magnesium sulphate ($MgSO_4$) solution for 90 days by weight of water. At the end of the duration of exposure, the specimens were weighed, and the change in the percentage of mass was determined in comparison to their initial mass using Eq. 5. Additionally, the SMB samples underwent a CS test. The findings were contrasted with the CS values of conventional masonry blocks, which were cured for 28 days without being exposed to sulfate conditions. Ultimately, the percentage decrease in strength was calculated using Eq. 6, as referenced in studies [39, 40].

3.3.8 Chloride attack

Masonry blocks exposed to certain environments are susceptible to chloride attack, as chloride ions can penetrate the binder. The resistance of SMB specimens to chloride attack was evaluated using a method similar to that employed for acid and sulphate attack tests. The samples were submerged in a 5% sodium chloride (NaCl) solution for 90 days by weight of water. Following the duration of exposure, the SMB samples were weighed, and the change in the percentage of mass was calculated in relation to their original mass using Eq. 5. Additionally, the SMB samples underwent a CS test. The outcomes were contrasted with the CS values of SMBs cured for 28 days without being exposed to chloride conditions. The percentage reduction in strength was then calculated using Eq. 6, as referenced in [37, 39].

3.3.9 Thermal conductivity

Thermal conductivity quantifies the heat transfer through concrete via conduction. The thermal conductivity test for SMB specimens with various C:A ratios was performed after 28 days of the curing period, following the guidelines of BS EN 12667:2001 [41]. The test utilized a heat flow meter technique and a guarded hot plate system with 2 disc specimens of the same mix ratios. The specimens for different mix ratios were prepared in the form of rounded discs having a thickness of 20 mm and a diameter of 180 mm. The thermal conductivity was evaluated by subjecting all masonry specimens of different C:A ratios to a temperature varying from 30 °C to 70 °C, with intervals of 10 °C.

3.3.10 Temperature resistance

Resistance of the SMBs to high temperatures after curing for 28 days was evaluated by keeping the samples in an electric furnace with a heating capacity of 1200 °C. The SMB specimens of different C:A ratios were exposed to different ranges of temperature from 200 °C to 800 °C, with 200 °C intervals, for two hours each. After the specified duration of heating, the SMB samples were removed and left to cool naturally. Subsequently, their weight and CS were measured. These values were then compared to the initial measurements taken from conventional masonry blocks prior to testing. Ultimately, the percentage change in mass and CS was calculated [39, 42].

3.3.11 Ultrasonic pulse velocity test

The Ultrasonic Pulse Velocity (UPV) test was conducted to evaluate the internal quality and homogeneity of SMBs, identifying potential defects such as cracks or voids. After 28 days of curing, UPV measurements were performed on 150 mm concrete cubes of various mix ratios using a Proceq Pundit PL-200 device with 54 kHz transducers, following ASTM C597 [43] and IS 516 (Part 5/Sec 1): 2018 [44]. Transducers were placed on opposite faces with a couplant gel, and calibration was done using a standard rod. Each sample was tested three times, and the average value was recorded for analysis.

3.3.12 Rapid chloride penetration test

The Rapid Chloride Penetration Test (RCPT) was conducted by following the procedure specified in ASTM C1202 [45]. The test specimens consisted of concrete discs with a diameter of 100 mm and a thickness of 50 mm, made from cylindrical specimens with a diameter of 100 mm and a height of 200 mm, representing different SMB concrete mix ratios. These specimens were cured in gunny bags for around 28 days. After curing, the specimens were trimmed with a water-cooled diamond saw. Three discs of 50 mm each were taken from the central part of the 200 mm cylinders, discarding the upper and lower portions. The curved surfaces of the 100 mm diameter discs were coated with epoxy or plastic after surface drying to ensure impermeability. The RCPT was conducted on SMB concrete specimens with

various mix ratios over 28 days, and the results for each test were the mean average of 3 specimens.

4 Results and discussion

4.1 Hardened density

The hardened density of SMBs across different mix proportions is shown in Table 4. The reported values reflect the average outcomes derived from three specimens per mix. The analysis revealed a decline in hardened density as the RCA content increased. For all mix ratios, the hardened density was lower compared to the 1:6 mix ratio, with reductions ranging from 1.75% to 9.77%. Specifically, the hardened density of SMBs decreased from 2243 kg/m3 for a C:A ratio of 1:6 to 2024 kg/m3 for a 1:24 ratio. Furthermore, within each C:A ratio, the hardened density showed a stepwise decrease, ranging from 0.98% to 1.75% compared to the preceding ratio. This reduction in density is significantly influenced by the properties of RCAs, such as their density and heterogeneity, which include particle size distribution, fines content, and the bonding efficiency of aggregates during the vibro-compaction process [46]. Higher mix ratios contribute to a lower bulk density, reduced specific gravity, and increased porosity, collectively leading to diminished hardened density. The results comply with the acceptance criteria specified in IS 2185 (Part 1)−2005 [31] and ASTM C90 [33], which require minimum densities of 1800 kg/m3 and 2000 kg/m3, respectively.

4.2 Compressive strength

The CS of SMBs with varying C:A ratio is presented in Table 4, highlighting both dry compressive strength (DCS) and wet compressive strength (WCS) after a curing period of 28 days. For the WCS assessment, the blocks were submerged in potable water for around 24 h prior to testing in a compression strength testing machine. The results indicated a decline in both DCS and WCS as RCA content increased, signifying that higher C:A ratios lead to reduced SMB strength. At higher C:A ratios, reduced cement content resulted in DCS reductions of 11.49% to 82.17% and WCS reductions of 14.25% to 86.27% compared to the 1:6 mix ratio. This strength loss is primarily attributed to reduced cement hydration product formation at higher ratios due to lower cement content, increased porosity, and the absorbent nature of RCAs.The CS of SMBs for C:A ratios from 1:6 to 1:24 ranged from 25.97 MPa to 3.35 MPa for both DCS and WCS. A gradual reduction in CS was observed for mixes from 1:6 to 1:15, with decreases ranging from 10.09% to 18.01%, while mixes from 1:18 to 1:24 exhibited more pronounced reductions, ranging from 15.74% to 56.21% compared to the previous ratio.

The WCS results were consistently lower than the DCS values due to water acting as a lubricant within the permeable pores, reducing the interparticle bonding resistance and increasing susceptibility to particle displacement [47]. The wet-to-dry CS ratio ranged from 0.94 to 0.72 for all the mix ratios. Mixes with lower C:A ratios, such as 1:6 and 1:8, exhibited smaller differences between WCS and DCS due to their higher cement content, which positively influenced strength. This higher cement content facilitated additional hydration of unreacted cement particles during immersion, partially offsetting the strength loss caused by water presence [48]. The results comply with the IS 2185 (Part 1)−2005 [31] standard, which requires a minimum CS of 5 MPa for load-bearing SMBs, achieved by mixes ranging from 1:6 to 1:21. Additionally, the ASTM C90 [33] standard, which specifies a minimum CS of 13.1 MPa, was satisfied by mix ratios of 1:6 to 1:13 under both wet and dry conditions for load-bearing SMBs.

The hardened density of SMBs is strongly correlated with their CS. An increase in density typically results in higher CS, whereas a reduction in density leads to a corresponding decrease in strength. The density of SMBs is primarily determined by the packing density or packing behaviour of the concrete during production. This packing behaviour influences the formation of pores or voids within the concrete and affects the block's strength and density. As illustrated in Fig. 3(a), regression analysis indicates that the relationship between hardened density and CS is best

Table 4 Physical and mechanical properties of SMBs with varying mix ratios

Mix ratio (C:A)	Hardened density in kg/m^3	Compressive strength in MPa		Flexural strength in MPa		Water absorption in %
		Dry	Wet	Dry	Wet	
1:6	2243	25.97	24.40	6.92	4.73	1.58
1:8	2204	22.99	20.92	5.37	3.59	1.93
1:11	2182	19.65	17.15	3.98	2.66	2.36
1:13	2161	17.41	14.78	3.22	2.16	2.79
1:15	2132	15.65	12.78	2.45	1.64	3.16
1:18	2095	13.19	10.27	1.98	1.33	3.54
1:21	2060	10.23	7.65	1.34	0.90	4.12
1:24	2024	4.63	3.35	0.92	0.62	4.51

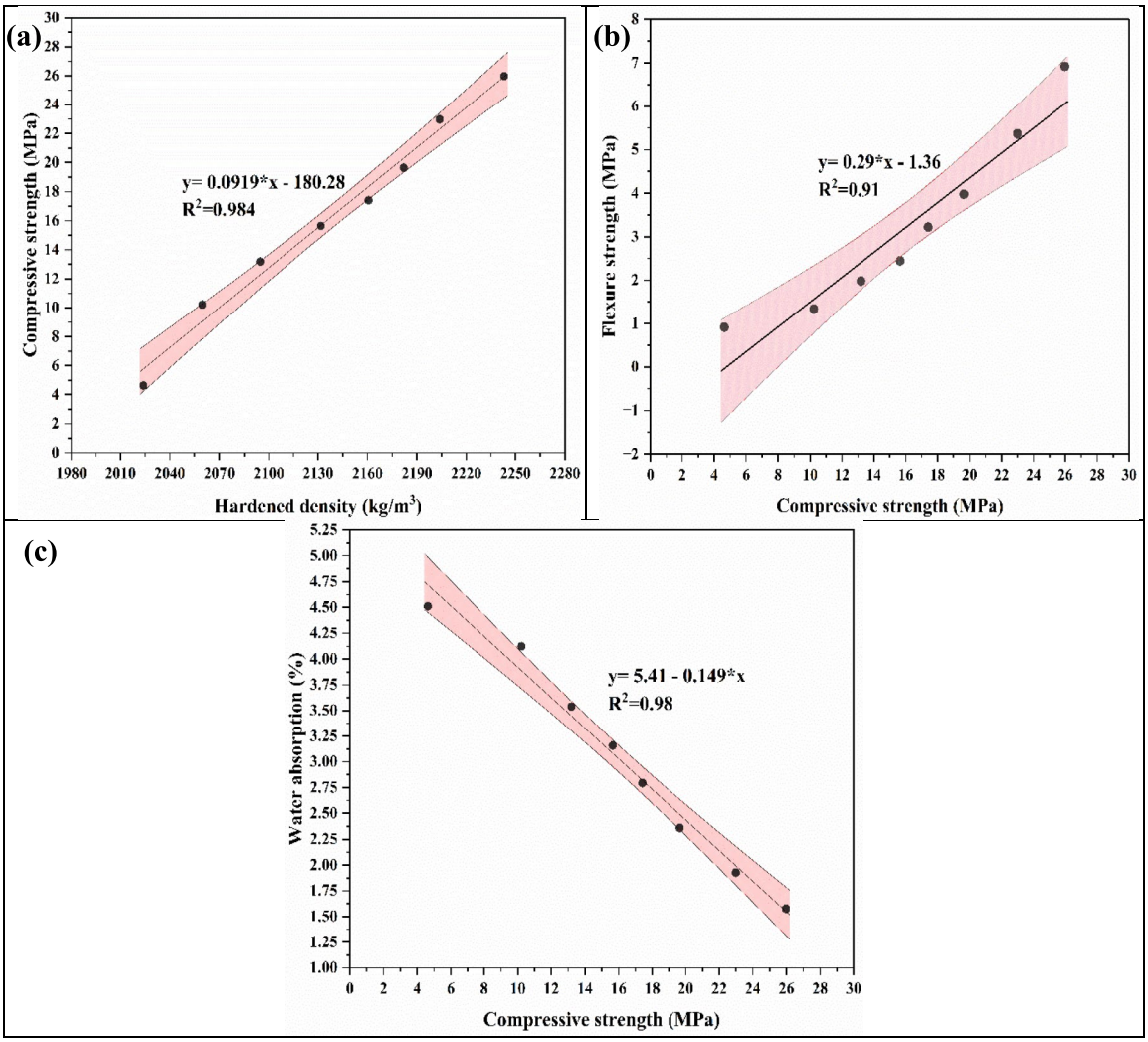


Fig. 3 Regression analysis results of SMBs: (**a**) Correlation between hardened density and CS; (**b**) Correlation between CS and FS; and (**c**) Correlation between CS and WA

represented by a linear function with a high correlation coefficient (R2) of 0.984.

4.3 Flexural strength

The FS results for the SMBs are tabulated in Table 4, representing the average of three measurements. These results exhibited a trend similar to that of CS, with both dry and wet FS values decreasing as the RCA content increased. For example, at higher C:A ratios, the reduction in cement content led to a decrease in dry FS by 22.46% to 86.72% and wet FS by 24.03% to 86.98% compared to the 1:6 mix ratio. The FS values of SMBs ranged from 6.92 MPa to 0.62 MPa across C:A ratios of 1:6 to 1:24 under both dry and wet conditions. Additionally, the FS declined with each successive mix ratio, with reductions ranging from 18.96% to 32.48%. Importantly, the FS of all block specimens significantly exceeded the requirement of 10% of the CS, as outlined by Dayaratnam, P (1987) [34], and complied with the standards specified in IS 4860–1968 [35].

The failure patterns of SMBs were predominantly marked by diagonal shear cracks caused by elevated local tensile stresses within the blocks. Vertical cracks were also observed at the centre of the blocks, which ultimately failed as the cracks branched out into diverging shear fractures. A regression analysis presented in Fig. 3(b) demonstrates a strong linear relationship between CS and FS, yielding a correlation coefficient (R2) of 0.91.

4.4 Water absorption

WA is a crucial property of masonry blocks, as it significantly affects their durability and the bond strength between the blocks and mortar in construction. Excessive WA can weaken the blocks by increasing porosity, which compromises their structural integrity and reduces strength.

Conversely, lower WA rates reflect higher-quality blocks that are more resistant to weathering and better maintain their structural integrity. Both the quality of the blocks and their bond with mortar are influenced by WA, thereby impacting the overall strength of the structure [49, 50]. For all mix ratios ranging from 1:6 to 1:24, the WA values varied between 1.58% and 4.51%. The percentage of WA for SMBs increased with each successive mix ratio, showing an increment of 9.40% to 22.41% compared to the previous ratio. This rise in WA at higher mix ratios can be attributed to the increased voids and the absorbent characteristics of RCAs. At higher mix ratios, the RCA content exceeded the cement content, leading to a weaker interfacial transition zone (ITZ) and higher WA in the blocks. The WA results, as shown in Table 4, confirm that all values remain well below the maximum allowable limit of 10%, as specified in IS 2185 (Part 1)–2005 [31]. Since the WA rates are within permissible limits, there is minimal impact on the strength, durability and long-term performance of the SMBs, ensuring that the structural integrity remains uncompromised.

The increased proportion of RCAs predominantly influences the WA properties of SMBs. Furthermore, the reduced cement content and the presence of adhered mortar on the surfaces of the aggregates contribute to higher WA in these blocks. A regression analysis, shown in Fig. 3(c), indicates that the strongest correlation between CS and WA is represented by a linear function with a high correlation coefficient (R2) of 0.98.

4.5 Sorptivity

The sorptivity values of SMBs for different C:A ratios are depicted in Fig. 4, presenting the rate of sorption per unit area of SMB discs as a function of the square root of time. The findings reveal that sorptivity increases progressively with higher C:A ratios, primarily due to a rise in void content, which enhances WA. SMBs with lower C:A ratios demonstrated significantly lower sorptivity compared to those with higher ratios. After six hours of sorption, the sorption rates per unit area were measured at 1.65 mm, 2.11 mm, 2.33 mm, 3.28 mm, 3.86 mm, 5.16 mm, 5.87 mm, and 6.39 mm for C:A ratios of 1:6, 1:8, 1:11, 1:13, 1:15, 1:18, 1:21, and 1:24, respectively. Following the final sorption stage, the recorded sorption rates per unit area were 4.15 mm, 5.23 mm, 5.35 mm, 5.94 mm, 6.18 mm, 6.69 mm, 6.81 mm, and 7.49 mm for the same C:A ratios. According to Uzoegbo [51] and Sathiparan N et al. [52] the sorptivity coefficient (in $mm/h^{0.5}$) is used to evaluate the quality of masonry blocks, with the following classifications: less than 6 mm is considered excellent, 6–12 mm is good, 12–15 mm is poor, and greater than 15 mm is very poor. Based on this classification, SMBs with C:A ratios of 1:6 to 1:13 fall into the excellent category, while those with ratios of 1:15 to 1:24 are categorized as good.

4.6 Acid attack

Acid attack, particularly from sulfuric acid, severely affects concrete SMBs through a dissolution mechanism. Acid infiltration into concrete leads to the dissolution of the cement

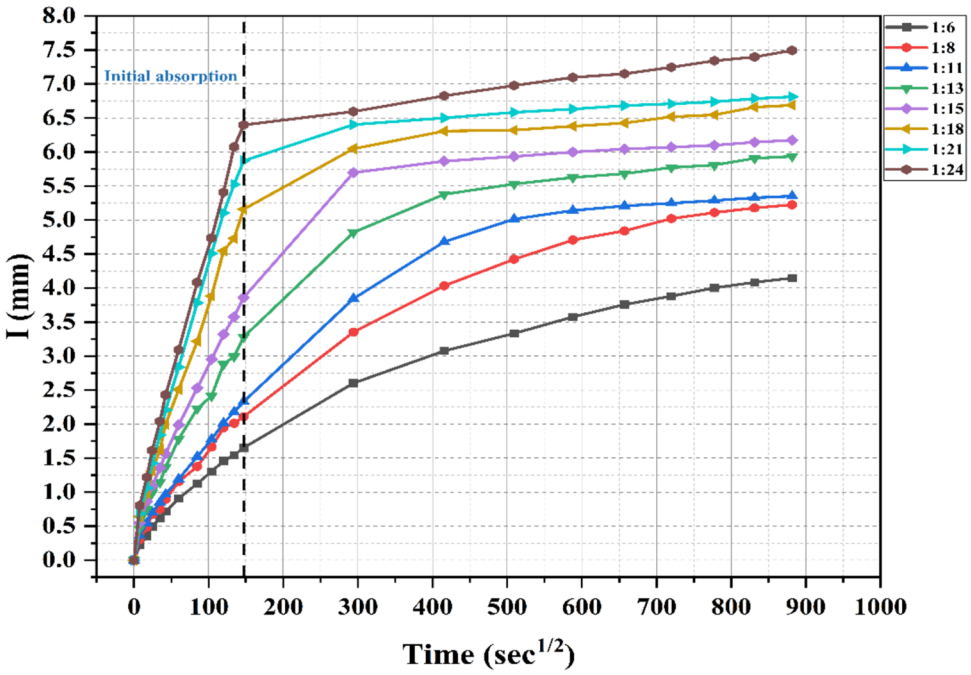


Fig. 4 Sorptivity of the SMBs for the different mix ratios

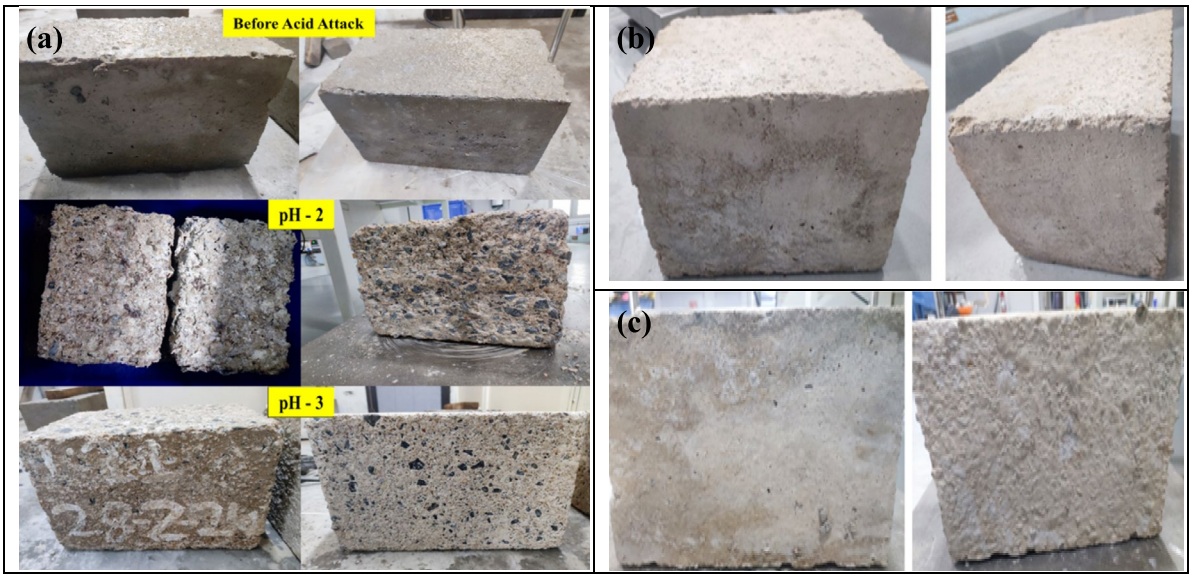


Fig. 5 (**a**) SMBs after sulphuric acid exposure; (**b**) SMBs after magnesium sulphate exposure; (**c**) SMBs after sodium chloride exposure

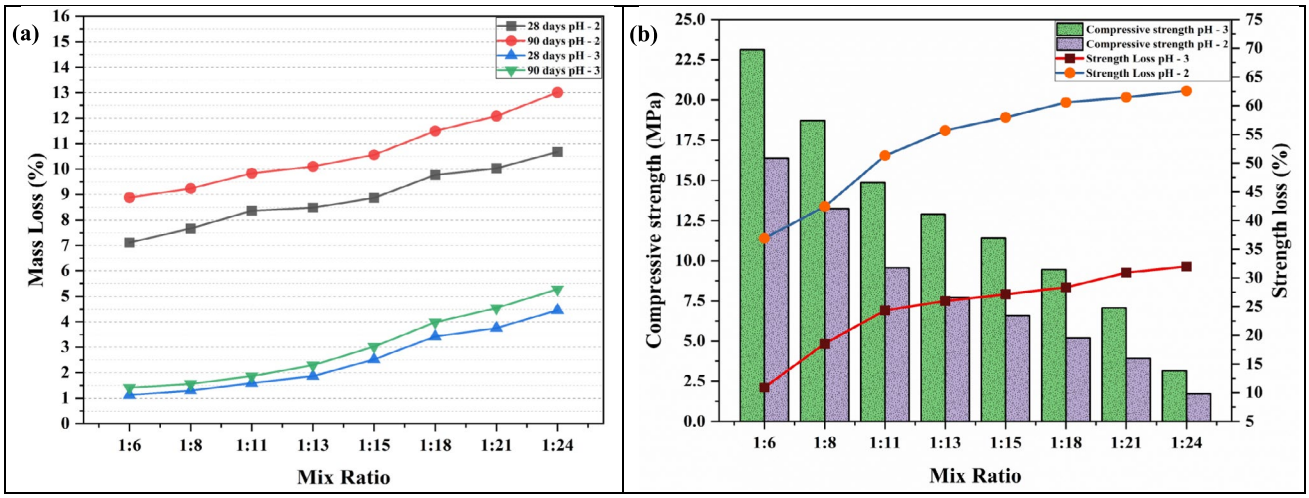


Fig. 6 (**a**) Percentage of mass loss in the SMBs after sulphuric acid exposure; (**b**) Strength loss of the SMBs after 90 days of sulphuric acid exposure

paste binder, resulting in the formation of soft, soluble gypsum. This gypsum interacts with water and tricalcium aluminate, leading to the development of expansive ettringite. The expansion caused by ettringite contributes to mass loss in acid-exposed concrete samples, creating tensile stresses that induce microcracks and spalling [53, 54]. Figure 5(a) depicts the deteriorated SMB specimens following exposure to acidic solutions with pH levels of 2 and 3 for 90 days. Visual inspection revealed significant surface degradation, including binder disintegration and aggregate exposure.

The mass changes in RAC SMBs due to acid immersion are illustrated in Fig. 6(a). It was observed that the mass of SMBs marginally diminished following 28 days of exposure to the acidic solution, with mass loss increasing after 90 days of acidic exposure for both pH conditions. Mass loss was more noted in SMBs subjected to a pH of 2 compared to those exposed to a pH of 3. For a pH of 3, mass loss ranged from 1.13% to 4.46% after 28 days and from 1.41% to 5.28% after 90 days for SMBs with C:A ratios from 1:6 to 1:24. In contrast, for a pH of 2, mass loss ranged from 7.11% to 10.67% after 28 days and from 8.89% to 13.02% after 90 days for the same C:A ratios. Sulfuric acid exhibits a high reactivity with calcium hydroxide [$Ca(OH)_2$], one of the principal products of cement hydration, resulting in the formation of soluble compounds such as calcium sulfate ($CaSO_4\ 2H_2O$). These reaction products are prone to leaching, which initiates structural deterioration in concrete. The presence of RCA tends to intensify this degradation process due to its inherent characteristics, including higher porosity, residual cementitious paste, and increased specific surface

area. These features facilitate acid penetration and enhance chemical reactivity, thereby accelerating the breakdown of cement matrix components. Consequently, concrete containing RCA is more susceptible to mass loss and mechanical strength reduction under sulfuric acid exposure [55]. The CS of RCA-based SMBs was assessed in accordance with ASTM standard procedures. Figure 6(b) illustrates the CS and the percentage strength loss of SMBs with various C:A ratios after 90 days of exposure to sulfuric acid. For mix ratios ranging from 1:6 to 1:24, the CS ranged from 23.13 MPa to 3.15 MPa at pH—3 and from 16.38 MPa to 1.73 MPa at pH—2. The strength loss after 90 days of sulfuric acid exposure was between 10.92% and 32.01% for a pH of 3 and between 36.92% and 62.59% for a pH of 2.

4.7 Sulfate attack

The effect of magnesium sulfate on SMBs was characterized by notable chemical degradation, resulting in mass loss and strength reduction. Visual observations of the blocks, as shown in Fig. 5(b), revealed slight deterioration in SMBs, including corner disintegration and surface damage after being exposed to magnesium sulfate solution for 90 days. The mass variations in SMBs due to sulfate attack are tabulated in Table 5. The results showed a slight reduction in mass after being immersed in the magnesium sulfate solution for 28 days, with a further increase in mass loss after being exposed to the solution for 90 days. The mass loss of SMBs exposed to magnesium sulfate ranged from 1.08% to 2.49% after 28 days and from 1.27% to 3.08% after 90 days for C:A ratios between 1:6 and 1:24. The CS of SMBs was evaluated following ASTM standard procedures. Table 5 presents the percentage strength loss of SMBs with different C:A ratios after 90 days of magnesium sulfate exposure. For mix ratios ranging from 1:6 to 1:24, CS values ranged from 23.45 MPa to 3.32 MPa after 90 days of exposure, with strength losses varying between 9.70% and 28.37%. The reduction in CS is directly related to the mass loss, suggesting that both factors play a substantial role in the overall performance of SMBs when subjected to sulfate attack. The results align with previous studies, indicating that an increase in recycled aggregate content leads to greater mass loss in concrete subjected to magnesium sulfate solutions. For instance, concrete with 100% recycled aggregate exhibited nearly double the mass loss compared to concrete with no recycled aggregate because of the lower density and higher porosity of RCA, which facilitates sulfate ingress and deterioration [56]. Additionally, the combination of increased RCA and reduced binder content leads to a compounded effect on durability and weakens the cement matrix and aggregate bond, increasing permeability and allowing sulfate ions to penetrate more easily, resulting in mass and strength loss in SMBs [57].

4.8 Chloride attack

Chloride diffusion in concrete causes chloride ions (Cl^-) to react with hydrated cement, forming corrosion byproducts. These accumulate in pores and cracks, worsening microcracks, weakening the ITZ, and resulting in mass and strength loss [58, 59]. Visual inspections of the blocks, depicted in Fig. 5(c), revealed effects comparable to those caused by sodium chloride attack. After 90 days of exposure to sodium chloride, SMBs exhibited slight deterioration, including salt deposition on the surface, corner disintegration, and surface damage. Other researchers have also shown similar findings on RAC blocks [54]. Changes in mass were analyzed by comparing the mass loss after 28 days of curing with SMBs subjected to 28 and 90 days of chloride exposure. Variations in mass over different exposure periods are shown in Table 5. The mass loss of SMBs exposed to sodium chloride ranged from 0.67% to 2.36% after 28 days and from 0.83% to 2.81% after 90 days for C:A ratios between 1:6 and 1:24. Sodium chloride can trigger chemical reactions in concrete, such as the leaching of calcium hydroxide and the formation of Friedel's salts, which weaken the concrete matrix and increase mass loss. The higher porosity of RCA compared to natural aggregates exacerbates these effects by facilitating greater penetration of sodium chloride ions, leading to more pronounced mass loss over time [60, 61]. The CS of SMBs

Table 5 Mass and strength loss of SMBs subjected to sulfate and chloride exposure

Mix ratio (C:A)	Sulfate attack			Chloride attack		
	Mass loss in %		Strength loss in %	Mass loss in %		Strength loss in %
	28 days	90 days		28 days	90 days	
1:6	1.08	1.27	9.70	0.67	0.83	6.37
1:8	1.34	1.63	10.82	1.03	1.24	7.99
1:11	1.69	2.06	16.82	1.47	1.73	10.41
1:13	1.86	2.30	19.12	1.56	1.92	11.55
1:15	2.11	2.48	24.40	1.70	2.05	15.57
1:18	2.19	2.61	25.45	1.80	2.12	18.88
1:21	2.39	2.92	26.11	1.95	2.37	20.29
1:24	2.49	3.08	28.37	2.36	2.81	23.01

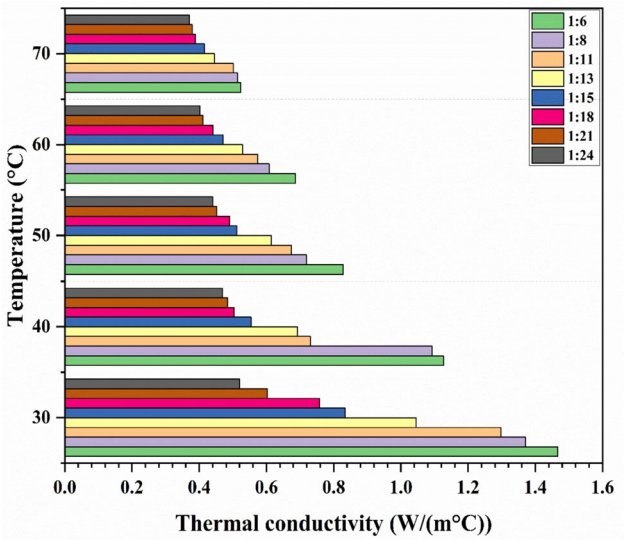


Fig. 7 Thermal conductivity characteristics of SMBs for different mixes

was tested to ensure compliance with ASTM standard procedures. Table 5 shows the percentage strength loss of SMBs with varying C:A ratios after 90 days of exposure to sodium chloride. For mix ratios ranging from 1:6 to 1:24, CS values ranged from 24.32 MPa to 3.57 MPa, with strength losses ranging between 6.37% and 23.01% after 90 days of exposure. The CS loss due to sodium chloride attack is generally proportional to the amount of RCA used. A higher RCA content often results in greater strength reductions, as the material's characteristics increase its susceptibility to salt-induced deterioration.

4.9 Thermal conductivity

The thermal conductivity of SMBs with varying C:A ratio is depicted in Fig. 7 in accordance with BS EN 12667:2001 [41] standards. Results indicate that thermal conductivity decreases as the C:A ratio increases. This behaviour is attributed to the relationship between thermal conductivity and density; a higher RCA content reduces the density of the concrete, leading to lower thermal conductivity. Previous studies have similarly reported that the concrete's thermal conductivity values are directly correlated with its density and the RCA content [62]. The thermal conductivity of SMBs decreases with both rising temperatures and increasing C:A ratios. At 30 °C, the thermal conductivity value ranges from 1.467 W/m°C to 0.521 W/m°C, while at approximately 70 °C, it varies between 0.523 W/m°C and 0.371 W/m°C for different C:A ratio SMBs. The proportionate decrease in thermal conductivity of SMBs at different temperatures compared to SMBs with a C:A ratio of 1:6 ranges from 1.62% to 64.51%.

4.10 Temperature resistance

Visual inspection of colour changes, spalling, and surface cracks is commonly recommended to assess the damage to RCA-based SMBs exposed to high temperatures. As shown in Fig. 8, the surfaces of SMBs exposed to temperatures up to 800 °C exhibited noticeable changes. At 400 °C, the surfaces of SMBs with different C:A ratios largely retained their original colour and appearance. Cracks began to appear at 600 °C, and at 800 °C, the spalling was witnessed,

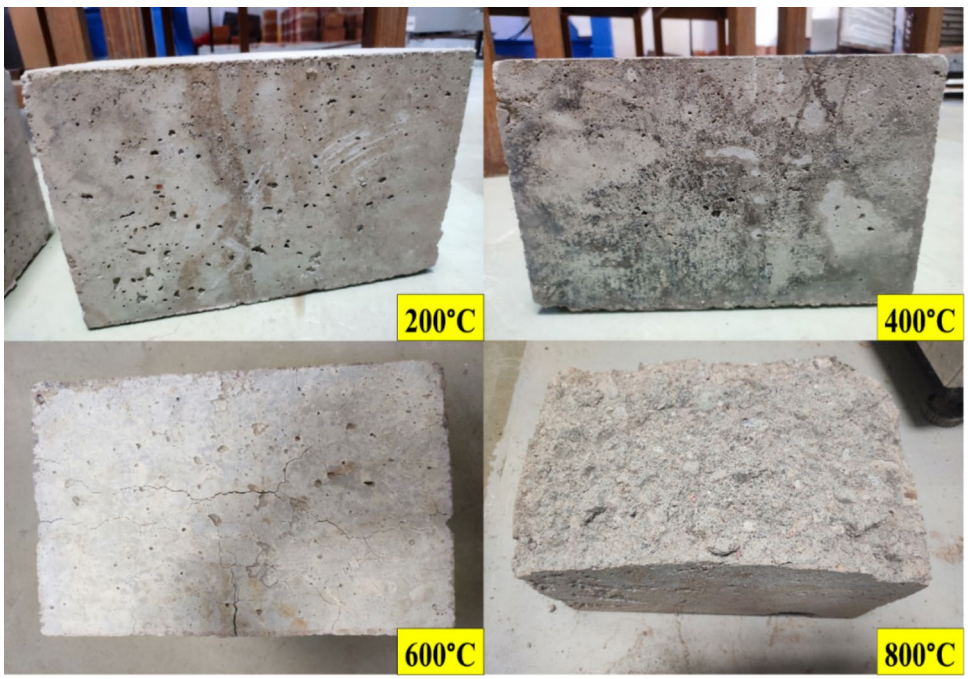


Fig. 8 The changes in SMB surfaces after being exposed to different temperatures

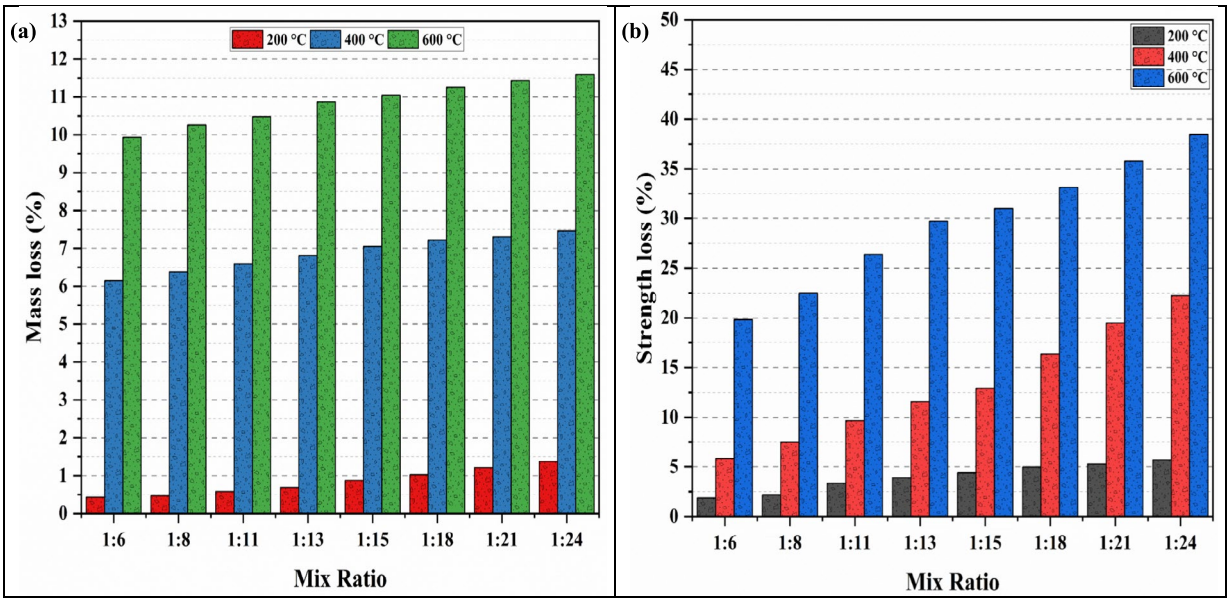


Fig. 9 (**a**) Mass loss of the SMBs after being exposed to different degrees of temperature; (**b**) Strength loss of the SMBs after being exposed to different degrees of temperature

likely due to pore pressure generation and crack transmission associated with spalling behaviour [39, 63].

Mass loss for the SMB samples increased progressively with rising temperatures, as depicted in Fig. 9(a). SMBs with different C:A ratios experienced mass losses ranging from 0.44% to 13.24% as the temperature rose from 200 °C to 800 °C. Blocks with higher C:A ratios exhibited greater mass loss, ranging from 0.58% to 13.24%, compared to those with a C:A ratio of 1:6. This mass loss is mainly because of the depletion of cement hydration products and the evaporation of free and confined water, particularly due to the degradation of calcium hydroxide ($Ca(OH)_2$). These findings align with observations from prior studies by Janotka and Nurnbergerova [64]. At 800 °C, significant mass loss occurred across all mixes, largely due to the evaporation of all absorbed water in the concrete, a phenomenon also noted by Ramesh et al.[65].

After heat treatment, the cooled SMB samples were tested for CS, with results shown in Fig. 9(b). All SMBs, regardless of C:A ratio, exhibited a progressive increase in strength loss at temperatures of 200 °C to 800 °C. Strength losses ranged from 1.87% to 5.69% at 200 °C, 5.85% to 22.25% at 400 °C, 19.84% to 38.44% at 600 °C, and 23.24% to 65.80% at 800 °C. The results presented in the figures primarily focus on SMBs exposed to temperatures up to 600 °C. It is because at 800 °C, all the blocks with different C:A ratios fractured into pieces, as depicted in Fig. 8. Blocks with lower C:A ratios demonstrated less strength loss compared to those with higher ratios at all temperature levels. The reduction in strength is primarily due to the water-vapour transition within the concrete's interlayers, which creates high internal pressures. Additionally, at elevated temperatures, aggregate expansion and cement paste shrinkage weaken the ITZ, and the bond between aggregates and cement paste, which combines with the decomposition of hydrated cement products, leads to significant degradation and strength reduction [66].

Table 6 UPV and RCPT test results of SMBs for different mix ratios

Mix ratio (C:A)	Ultrasonic pulse velocity in m/s	Rapid chloride penetration in coulomb
1:6	3722.50	792.48
1:8	3564.25	982.35
1:11	3406.00	1058.23
1:13	3369.75	1675.78
1:15	3333.50	2121.12
1:18	3166.75	3088.17
1:21	3005.00	4449.64
1:24	2785.00	4904.64

4.11 Ultrasonic pulse velocity test

Table 6 presents the tabulated UPV test results for SMBs with varying C:A ratios. For each specimen, three individual readings were recorded, and the average UPV was calculated. The data in Table 6 indicates that SMBs with higher C:A ratios exhibited lower UPV values compared to those with lower C:A ratios. The average UPV for masonry blocks with C:A ratios ranging from 1:6 to 1:24 was between 3722.5 ± 186 m/s and 2785 ± 139 m/s, respectively. The reduction in UPV values at higher C:A ratios can be

primarily attributed to the increased void content or porosity in the blocks, resulting from the lower packing density of SMBs with higher C:A ratios.

The UPV of SMBs shows a strong linear correlation with both CS and hardened density. Higher UPV values indicate greater strength and density, largely influenced by the packing density of the concrete, which affects internal void formation. Regression analysis demonstrates a strong linear relationship, with correlation coefficients of R2 = 0.98 for UPV-CS and R2 = 0.97 for UPV-density, highlighting the reliability of UPV as an indicator of concrete quality in SMBs, as shown in Fig. 10(a) and (b).

4.12 Rapid chloride penetration test

The RCPT for SMBs was conducted in accordance with ASTM C1202 [45], focusing on various C:A ratios after a 28-day curing period. The RCPT values were assessed for C:A ratios ranging from 1:6 to 1:24, with the results shown in Table 6. The measured RCPT values varied between 792.48 C and 4904.64 C for these ratios. This test was performed to evaluate the accuracy and performance of the results, ensuring their direct correlation with those obtained from the UPV test. The RCPT and UPV tests provide complementary insights, with the RCPT value generally increasing as the UPV value decreases and vice versa. The packing density of the concrete significantly influences the UPV values of masonry blocks during block production. This packing behaviour, which impacts the formation of voids or pores within the concrete, plays a crucial role in determining both the UPV and RCPT values. A regression analysis presented in Fig. 10(c) reveals a strong linear correlation between UPV and RCPT, with a correlation coefficient (R2) of 0.92, indicating a robust relationship.

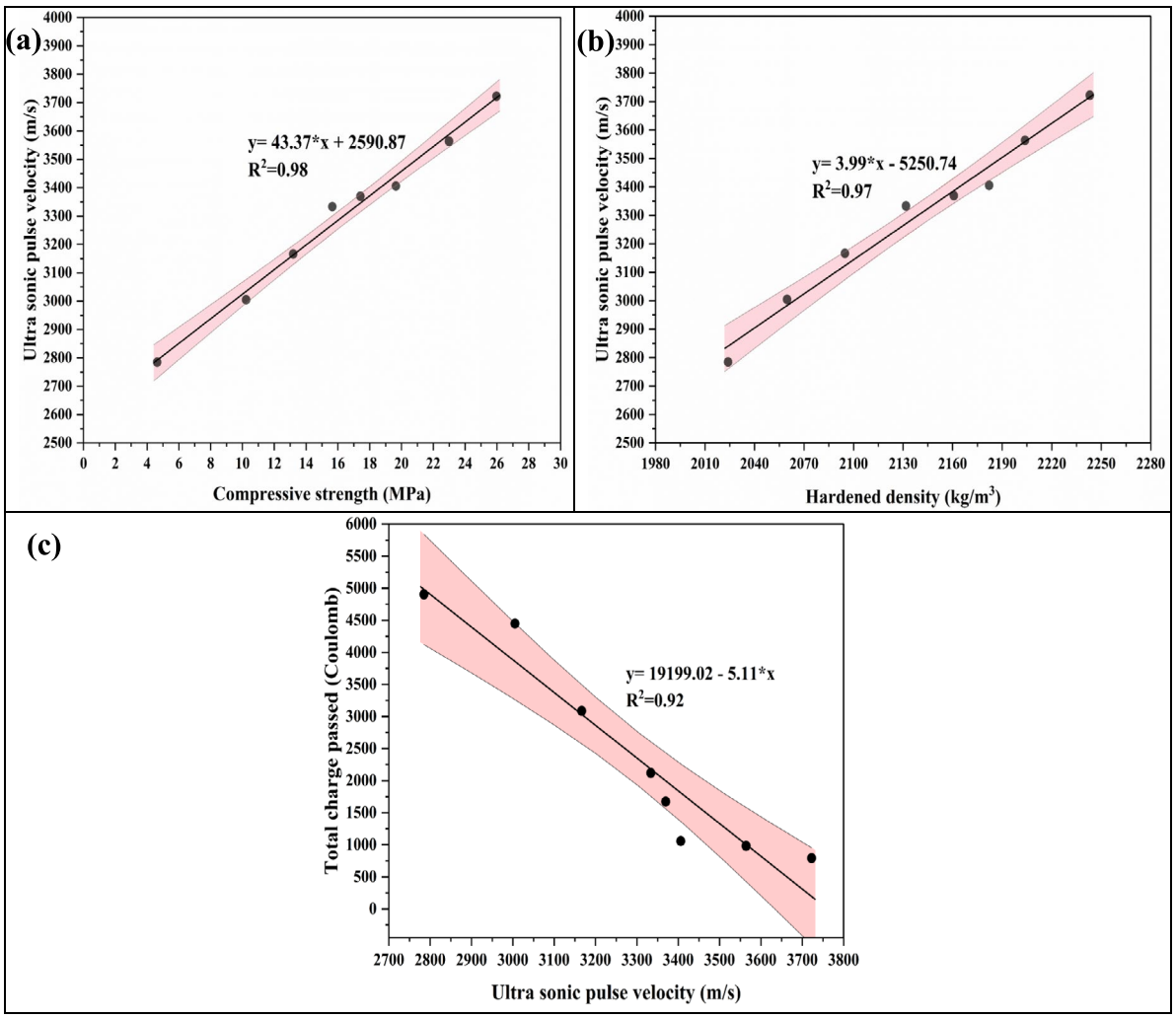


Fig. 10 Regression analysis results of SMBs: (**a**) Correlation between CS and UPV; (**b**) Correlation between hardened density and UPV; and (**c**) Correlation between UPV and RCPT

5 Microstructure properties

5.1 SEM

The SEM analysis of SMBs with different C:A ratios, as shown in Fig. 11 [32], reveals a consistent trend: increasing the C:A ratio results in a less dense and more porous microstructure. This is primarily due to the reduced cement content, which limits the formation of hydration products, particularly calcium silicate hydrate (C-S–H) gel, negatively impacting the mechanical behaviour of the blocks.

Figure 11(a), representing the 1:6 mix, shows a compact and homogeneous microstructure without visible pores, cracks, or unreacted cement particles. This dense matrix corresponds to the highest compressive strength values (DCS and WCS), reaching 25.97 MPa. The slight difference between dry and wet strengths (wet-to-dry ratio of 0.94) suggests effective hydration and a cohesive internal structure. Durability assessments under acidic exposure further validate its superior performance, with minimal mass losses (1.41% at pH < 3.0 and 8.89% at pH < 2.0) and moderate strength reductions (10.92% and 36.92%, respectively). The dense microstructure effectively limits acid infiltration and reduces the leaching of calcium compounds.

In contrast, Figs. 11(b) and (c), representing 1:11 and 1:15 mixes, display higher porosity, micro-voids, and unhydrated

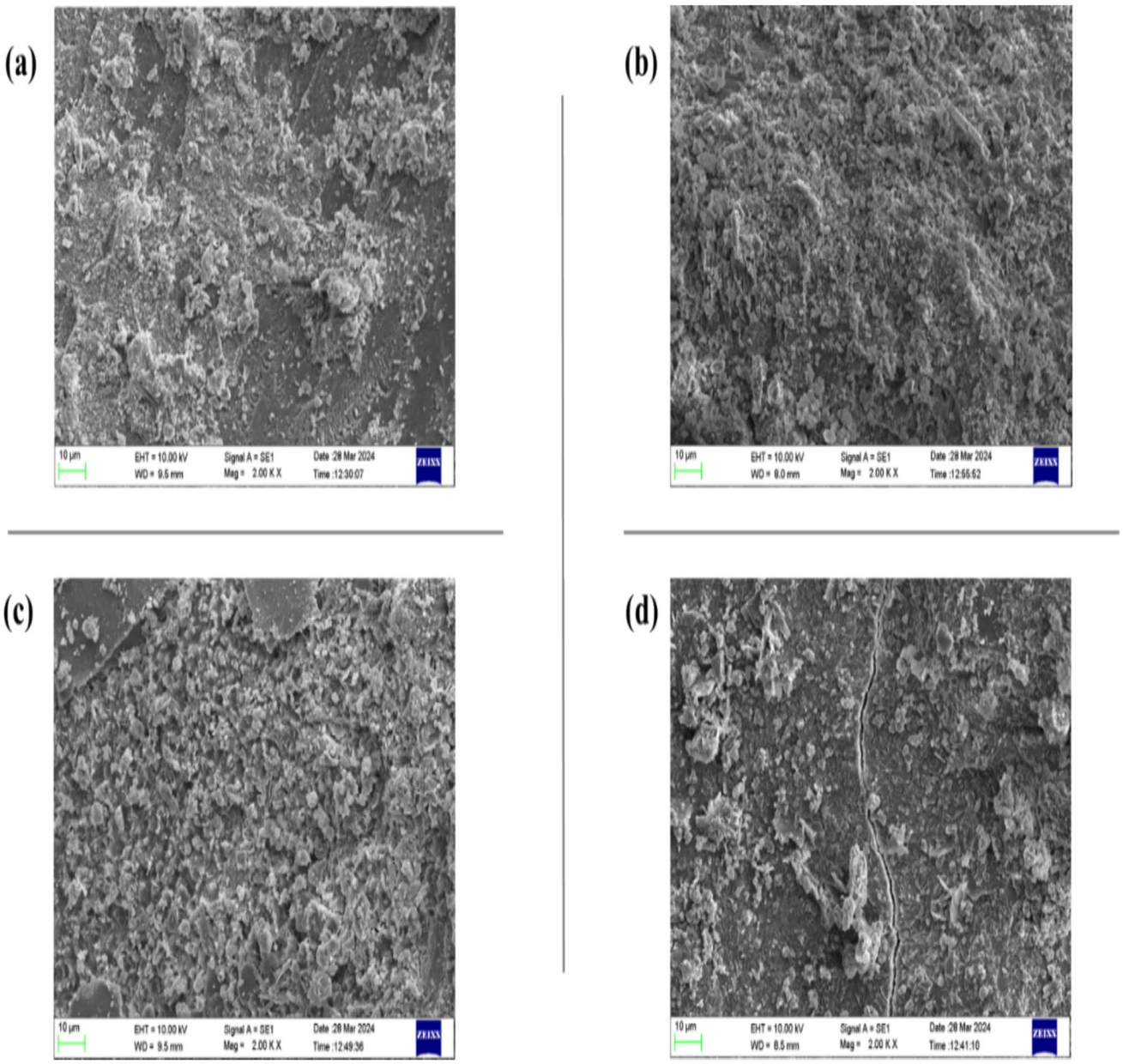


Fig. 11 SEM of SMB made of mix ratio (**a**) 1:6; (**b**) 1:11; (**c**) 1:15; (**d**) 1:21 [32]

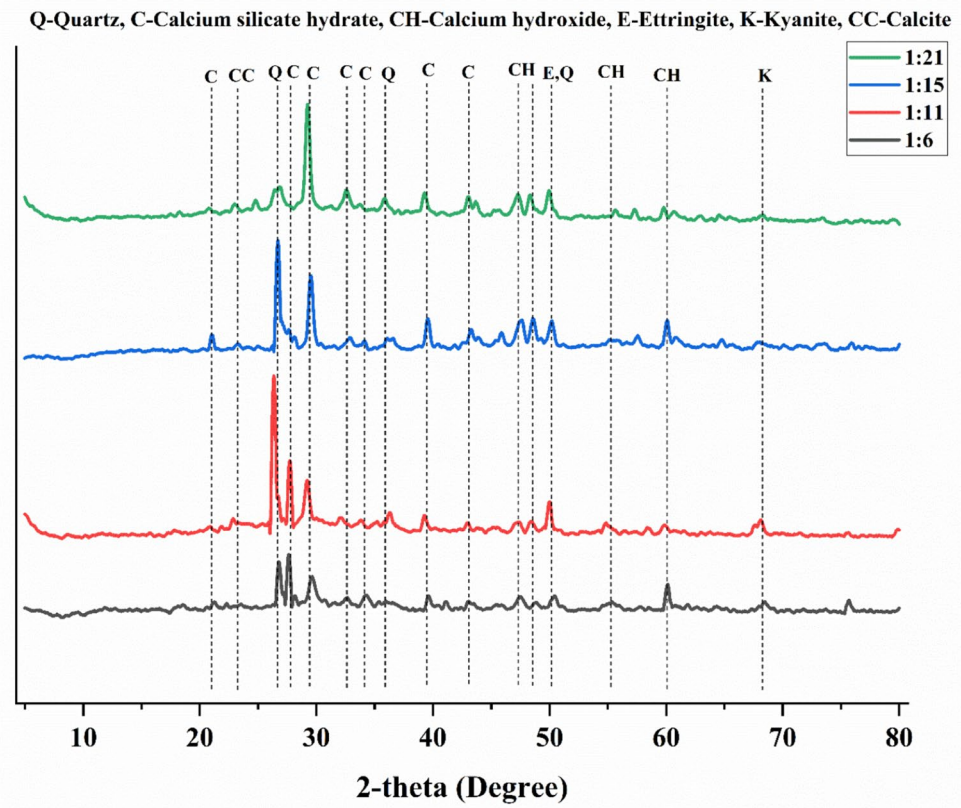


Fig. 12 XRD of SMBs made of mix ratios 1:6, 1:11, 1:15, and 1:21

cement particles. These features contribute to a significant decrease in strength—by 11.49% to 18.01% relative to the 1:6 mix—and increased water absorption. The porous structure facilitates acid ingress, accelerating the degradation of hydration products and compromising durability. The most severe microstructural damage is evident in Fig. 11(d) for the 1:21 mix, which shows prominent macrocracks and abundant unreacted cement grains. This results in a drastic decline in mechanical strength, with DCS and WCS reduced by 82.17% and 86.27%, respectively, compared to the 1:6 mix. Additionally, this mix experienced the highest mass losses after acid exposure.

Overall, increasing the C:A ratio leads to a progressive deterioration in microstructure, mechanical performance, and acid resistance. In contrast, lower C:A ratios yield denser, more cohesive matrices that enhance strength and chemical durability. These observations are consistent with findings by Pengfei Ren et al. [67] and Rahul Singh et al. [9], highlighting the critical role of adequate binder content in ensuring the structural integrity and longevity of SMBs under aggressive conditions.

5.2 XRD

The X-ray diffraction (XRD) patterns of all the SMB mixes are shown in Fig. 12. Analysis of these patterns indicates that the incorporation of RCA did not lead to significant changes in the mineralogical composition of the mixes. The predominant mineral phases identified across all mixes include quartz, calcite, calcium hydroxide, ettringite, kyanite, and calcium silicate hydrate (C–S–H). Quartz is primarily associated with the presence of natural sand and aggregates, while the peaks for calcite, calcium hydroxide, and ettringite correspond to cement hydration products. The presence of C–S–H, a crucial hydration product contributing to strength and durability, confirms the ongoing hydration reactions and suggests that RCA did not hinder the formation of this vital compound. Although kyanite was detected in minor quantities, it still contributed to the overall mineralogical profile. The consistency of the mineral phases, with only slight variations in peak intensities, further supports the conclusion that RCA, used as a secondary material, did not interfere with hydration processes or the development of key binding phases. These observations are consistent with previous studies on concrete prepared using OPC and a combination of natural and artificial aggregates [68].

Despite the similarity in XRD patterns, the physical and mechanical properties of the blocks showed a clear dependency on the RCA content. The mix with a 1:6 ratio demonstrated the most favourable performance, including higher compressive strength, reduced water absorption, and improved durability. In contrast, mix ratios of 1:11, 1:15, and 1:21 exhibited a gradual decline in performance metrics as the RCA content increased. This discrepancy between

mineralogical consistency and mechanical performance can be attributed to the fact that XRD peak intensities do not directly reflect structural properties. Instead, the effectiveness of hydration product formation, particularly C–S–H, calcium hydroxide (CH), and ettringite, plays a more critical role in determining the structural integrity of the material. While hydration products were present across all mixes, higher RCA content likely caused a dilution effect, limiting the formation of new hydrated phases and weakening the microstructure. Notably, a significant reduction in the quartz peak intensity was observed in the 1:21 mix, suggesting possible mineral transformation under experimental conditions. It may be due to enhanced interactions between quartz and reactive components, potentially promoting pozzolanic reactions and the consumption of amorphous silica, leading to the formation of secondary hydration products such as C–S–H gels. These transformations could account for the observed decline in quartz peak intensity and the associated decrease in mechanical performance. These insights underscore the necessity of combining mineralogical analysis with performance-based evaluations when assessing the suitability of RCA in masonry block production.

It can also be noted that the lower intensity in the 1:6 mix is a result of its higher binder content, which leads to the formation of more amorphous phases (like C-S–H gel) that naturally produce weaker diffraction peaks. On the other hand, the 1:21 mix's pattern appears slightly unusual because of the lower binder content, which results in less formation of hydration products like C-S–H. In contrast, the 1:11 and 1:15 mixes strike a better balance between binder and aggregate, which is why their XRD curves appear more distinct and well-defined.

6 Conclusions

This study focused on producing load-bearing solid masonry blocks using 100% recycled concrete aggregates and experimentally evaluating their strength and durability characteristics. The commercial production of such blocks has the potential to alleviate the demand for natural aggregate resources while mitigating environmental pollution associated with construction and demolition waste. Based on the analysis of the experimental findings related to the strength and durability performance of the recycled concrete aggregate solid masonry blocks, the following conclusions were derived:

1. The compressive and flexural strengths of the blocks declined as recycled concrete aggregate content increased and cement content decreased under both dry and wet conditions. However, mixes up to a 1:21 ratio continued to meet the strength requirements as per Indian standards for load-bearing applications, indicating sufficient mechanical performance under environmental stress.
2. Water absorption and sorptivity increased with higher recycled concrete aggregate content as the cement-to-aggregate ratio increased from 1:6 to 1:24, reflecting the porous nature and adhered mortar of recycled aggregates. Despite the higher values, all measurements remained within the permissible limits of Indian standards, confirming the acceptable moisture-related durability of the blocks.
3. Solid masonry blocks with higher recycled concrete aggregate content exhibited increased mass and strength loss as the cement-to-aggregate ratio increased from 1:6 to 1:24 when exposed to sulfuric acid, magnesium sulfate, and sodium chloride after 90 days. The deterioration was more pronounced at higher cement-to-aggregate ratios due to elevated porosity and weaker matrix-aggregate bonds, indicating reduced resistance to aggressive chemical environments.
4. Elevated temperatures ranging from 200 °C to 800 °C resulted in progressive mass and strength loss, particularly in blocks with higher recycled concrete aggregate content and lower binder levels. The degradation was primarily due to the decomposition of hydration products and increased internal pore pressure, demonstrating the impact of RCA on thermal stability. Mass loss ranged from 0.44% to 13.24%, while strength loss varied between 1.87% to 65.80% across this temperature range.
5. Thermal conductivity reduced with increasing recycled concrete aggregate content, ranging from 2.58% to 43.65%, across successive mixes at various temperatures, indicating improved thermal insulation properties. This characteristic supports the use of recycled concrete aggregate-based blocks in thermally efficient building envelopes.
6. Considering the combined effects of mechanical, thermal, and durability, a cement-to-aggregate ratio of up to 1:18 is recommended for producing structurally reliable, load-bearing masonry blocks using recycled concrete aggregates.

Acknowledgements The authors have not received funding or financial support to conduct research and/or prepare the article.

Author contributions Md Mohsin M Dafedar: Writing the original draft, Investigation, Visualization, software, Methodology, Data curation, and Conceptualizations. Balakrishna Rao K: Supervision, Conceptualization, review & editing. B.H.Venkataram Pai: Supervision, Conceptualization. Gopal Bharamappa Bekkeri: Data curation, Methodology. Kiran K Shetty: Supervision, review & editing, Methodology.

Funding Open access funding provided by Manipal Academy of Higher Education, Manipal. The authors declare that no funds, grants, or other support were received during the preparation of the manuscript.

Data availability All data available in the study.

Declarations

Ethical approval This paper neither was published nor is under review elsewhere.

Informed consent All the authors are aware of this paper.

Conflict of interest The authors have no relevant financial or non-financial interests to disclose.

Open Access This article is licensed under a Creative Commons Attribution 4.0 International License, which permits use, sharing, adaptation, distribution and reproduction in any medium or format, as long as you give appropriate credit to the original author(s) and the source, provide a link to the Creative Commons licence, and indicate if changes were made. The images or other third party material in this article are included in the article's Creative Commons licence, unless indicated otherwise in a credit line to the material. If material is not included in the article's Creative Commons licence and your intended use is not permitted by statutory regulation or exceeds the permitted use, you will need to obtain permission directly from the copyright holder. To view a copy of this licence, visit http://creativecommons.org/licenses/by/4.0/.

References

1. W. Luo, S. Liu, Y. Hu, D. Hu, K.W. Kow, C. Pang, B. Li, Sustainable reuse of excavated soil and recycled concrete aggregate in manufacturing concrete blocks. Constr. Build. Mater. **342**, 127917 (2022). https://doi.org/10.1016/j.conbuildmat.2022.127917
2. F. Belaïd, How does concrete and cement industry transformation contribute to mitigating climate change challenges? Resour. Conserv. Recycl. Adv. **15**, 200084 (2022). https://doi.org/10.1016/j.rcradv.2022.200084
3. B. Zhang, Y. Feng, J. Xie, J. Dai, W. Chen, Z. Xue, L. Li, Y. Li, J. Li, Effects of pretreated recycled powder substitution on mechanical properties and microstructures of alkali-activated cement. Constr. Build. Mater. **406**, 133360 (2023). https://doi.org/10.1016/j.conbuildmat.2023.133360
4. W. Ahmad, A. Ahmad, K.A. Ostrowski, F. Aslam, P. Joyklad, A scientometric review of waste material utilization in concrete for sustainable construction. Case Stud. Constr. Mater. **15**, e00683 (2021). https://doi.org/10.1016/j.cscm.2021.e00683
5. M.U. Hossain, C.S. Poon, I.M.C. Lo, J.C.P. Cheng, Comparative environmental evaluation of aggregate production from recycled waste materials and virgin sources by LCA. Resour. Conserv. Recycl. **109**, 67–77 (2016). https://doi.org/10.1016/j.resconrec.2016.02.009
6. L. Lu, Optimal replacement ratio of recycled concrete aggregate balancing mechanical performance with sustainability: a review. Buildings **14**(7), 2204 (2024). https://doi.org/10.3390/buildings14072204
7. S.V. Patil, K.B. Rao, G. Nayak, Influence of silica fume on mechanical properties and microhardness of interfacial transition zone of different recycled aggregate concretes. Adv. Civ. Eng. Mater. **10**, 20210011 (2021). https://doi.org/10.1520/ACEM20210011
8. M. Nedeljković, J. Visser, B. Šavija, S. Valcke, E. Schlangen, Use of fine recycled concrete aggregates in concrete: a critical review. J. Build. Eng. **38**, 102196 (2021). https://doi.org/10.1016/j.jobe.2021.102196
9. R. Singh, D. Nayak, A. Pandey, R. Kumar, V. Kumar, Effects of recycled fine aggregates on properties of concrete containing natural or recycled coarse aggregates: a comparative study. J. Build. Eng. **45**, 103442 (2022). https://doi.org/10.1016/j.jobe.2021.103442
10. J. Li, H. Zhou, W. Chen, Z. Chen, Mechanical properties of a new type recycled aggregate concrete interlocking hollow block masonry. Sustainability (Switzerland) **13**, 1–15 (2021). https://doi.org/10.3390/su13020745
11. J. Saravanan, P.V. Rao, Past investigations on development of sustainable bricks – A comprehensive review. Sustain. Chem. Environ. **3**, 100030 (2023). https://doi.org/10.1016/j.scenv.2023.100030
12. K. Prashanth, N.R. Lohith, V. M, S.M. Basutkar, Properties of fiber incorporated concrete blocks manufactured using recycled aggregates. Low-carbon Mater. Green Constr. **2**(1), 3 (2024). https://doi.org/10.1007/s44242-024-00034-w
13. K. Hu, S.T.A. Gillani, X. Tao, J. Tariq, D. Chen, Eco-friendly construction: Integrating demolition waste into concrete masonry blocks for sustainable development. Constr. Build. Mater. **460**, 139797 (2025). https://doi.org/10.1016/j.conbuildmat.2024.139797
14. N. Chan, C. Young-Rojanschi, S. Li, Effect of water-to-cement ratio and curing method on the strength, shrinkage and slump of the biosand filter concrete body. Water Sci. Technol. **77**, 1744–1750 (2018). https://doi.org/10.2166/wst.2018.063
15. C.S. Poon, S.C. Kou, L. Lam, Use of recycled aggregates in molded concrete bricks and blocks (2002). https://doi.org/10.1016/S0950-0618(02)00019-3
16. C.S. Poon, C.S. Lam, The effect of aggregate-to-cement ratio and types of aggregates on the properties of precast concrete blocks. Cem. Concr. Compos. **30**, 283–289 (2008). https://doi.org/10.1016/j.cemconcomp.2007.10.005
17. C.S. Poon, S. Kou, H. Wan, M. Etxeberria, Properties of concrete blocks prepared with low grade recycled aggregates. Waste Manag. **29**, 2369–2377 (2009). https://doi.org/10.1016/j.wasman.2009.02.018
18. Z. Guo, A. Tu, C. Chen, D.E. Lehman, Mechanical properties, durability, and life-cycle assessment of concrete building blocks incorporating recycled concrete aggregates. J. Clean. Prod. **199**, 136–149 (2018). https://doi.org/10.1016/j.jclepro.2018.07.069
19. A. Juan-Valdés, D. Rodríguez-Robles, J. García-González, M.I.S. de Rojas, M.I. Guerra-Romero, R. Martínez-García, J.M. Morán-Del Pozo, Recycled precast concrete kerbs and paving blocks, a technically viable option for footways. Materials **14**(22), 7007 (2021). https://doi.org/10.3390/ma14227007
20. X. Wang, C.S. Chin, J. Xia, Study on the properties variation of recycled concrete paving block containing multiple waste materials. Case Stud. Constr. Mater. **18**, e01803 (2023). https://doi.org/10.1016/j.cscm.2022.e01803
21. C.S. Poon, D. Chan, Effects of contaminants on the properties of concrete paving blocks prepared with recycled concrete aggregates. Constr. Build. Mater. **21**, 164–175 (2007). https://doi.org/10.1016/j.conbuildmat.2005.06.031
22. Bureau of Indian Standards IS 269, Ordinary portland cement – specification (2015). http://www.standardsbis.in
23. Bureau of Indian Standards IS 383, Coarse and fine aggregate for concrete – specification (2016). http://www.standardsbis.in

24. Bureau of Indian Standards IS 2386–3, Methods of test for aggregates for concrete, part 3: specific gravity, density, voids, absorption and bulking (1963). http://www.standardsbis.in
25. Bureau of Indian Standards IS 2386–4, Methods of test for aggregates for concrete, part 4: mechanical properties (1963). http://www.standardsbis.in
26. Bureau of Indian Standards IS 2386–1, Methods of test for aggregates for concrete, part 1: particle size and shape (1963).http://www.standardsbis.in
27. Bureau of Indian Standards IS 456, Plain and reinforced concrete – code of practice (2000). http://www.standardsbis.in
28. R.K. Dhir, H. Fict, M.C. Limbachiya, Suitability of recycled concrete aggregate for use in BS 5328 designated mixes. Struct. Build. **134**, 257–274 (1999). https://doi.org/10.1680/istbu.1999.31568
29. M.C. Limbachiya, E. Marrocchino, A. Koulouris, Chemical-mineralogical characterization of coarse recycled concrete aggregate. Waste Manag. **27**, 201–208 (2007). https://doi.org/10.1016/j.wasman.2006.01.005
30. B. Zhang, Y. Feng, J. Xie, W. Chen, Z. Xue, G. Zhao, Y. Li, J. Li, J. Yang, Compressive behaviour and microstructures of concrete incorporating pretreated recycled powder/aggregates: the coupling effects of calcination and carbonization. J. Build. Eng. **68**, 106158 (2023). https://doi.org/10.1016/j.jobe.2023.106158
31. Bureau of Indian Standards IS 2185: Part 1, Concrete masonry units – specification, part 1: hollow and solid concrete blocks (2005). http://www.standardsbis.in
32. M.M.M. Dafedar, K.B. Rao, B.H.V. Pai, G.B. Bekkeri, Evaluation of the engineering properties and sustainability of solid masonry blocks produced with recycled concrete aggregates. Innov. Infrastruct. Solutions **9**(11), 449 (2024). https://doi.org/10.1007/s41062-024-01720-1
33. ASTM C90–09, Standard specification for load bearing concrete masonry units (2009). http://www.astm.org
34. P. Dayaratnam, Brick and reinforced brick structures. In: New Delhi: South Asia Books. ISBN: 978–93–881–7820–4 (1987)
35. Bureau of Indian Standards IS 4860, Specification for acid-resistant bricks (1968). http://www.standardsbis.in
36. ASTM C1585- 04, Standard test method for measurement of rate of absorption of water by hydraulic-cement concretes (2007). http://www.astm.org
37. K. Sundaralingam, A. Peiris, A. Anburuvel, N. Sathiparan, Quarry dust as river sand replacement in cement masonry blocks: effect on mechanical and durability characteristics. Materialia (Oxf) **21**, 101324 (2022). https://doi.org/10.1016/j.mtla.2022.101324
38. ASTM C1898–20, Standard test methods for determining the chemical resistance of concrete products to acid attack (2020). http://www.astm.org
39. G.B. Bekkeri, K.K. Shetty, G. Nayak, K.A.A. Kumar, Durability performance of concrete incorporated with alkali-activated artificial aggregates. Emergent Mater (2024). https://doi.org/10.1007/s42247-024-00855-2
40. J. Wu, W. Zhu, J. Wei, M. Tang, S. Zhang, X. Zhang. A comparable study on the deterioration of concrete under sodium sulfate and magnesium sulfate attack. In: IOP Conference series: earth and environmental science. IOP Publishing Ltd (2021). https://doi.org/10.1088/1755-1315/787/1/012037
41. British Standards Institution BS EN 12667-, Thermal performance of building materials and products: determination of thermal resistance by means of guarded hot plate and heat flow meter methods: products of high and medium thermal resistance (2001). http://www.bsigroup.com
42. J.O. Ukpata, D.E. Ewa, J.U. Liwhuliwhe, G.U. Alaneme, K.E. Obeten, Effects of elevated temperatures on the mechanical properties of laterized concrete. Sci Rep **13**(1), 18358 (2023). https://doi.org/10.1038/s41598-023-45591-5
43. ASTM C597–02, Standard test method for pulse velocity through concrete (2003). http://www.astm.org
44. Bureau of Indian Standards IS 516 (Part 5/Sec 1), Hardened concrete - methods of test - part 5 non-destructive testing of concrete section 1 ultrasonic pulse velocity testing (2018). http://www.standardsbis.in
45. ASTM C1202 – 12, Standard test method for electrical indication of concrete's ability to resist chloride ion penetration (2012). http://www.astm.org
46. M. Martín-Morales, G.M. Cuenca-Moyano, I. Valverde-Espinosa, I. Valverde-Palacios, Effect of recycled aggregate on physical-mechanical properties and durability of vibro-compacted dry-mixed concrete hollow blocks. Constr. Build. Mater. **145**, 303–310 (2017). https://doi.org/10.1016/j.conbuildmat.2017.04.013
47. T.E. Elahi, A.R. Shahriar, M.S. Islam, Engineering characteristics of compressed earth blocks stabilized with cement and fly ash. Constr. Build. Mater. **277**, 122367 (2021). https://doi.org/10.1016/j.conbuildmat.2021.122367
48. H.B. Nagaraj, A. Rajesh, M.V. Sravan, Influence of soil gradation, proportion and combination of admixtures on the properties and durability of csebs. Constr. Build. Mater. **110**, 135–144 (2016). https://doi.org/10.1016/j.conbuildmat.2016.02.023
49. B.H.A. Bakar, S. Saari, N.A. Surip, Water absorption characteristic of interlocking compressed earth brick units. In: AIP conference proceedings. American institute of physics Inc (2017). https://doi.org/10.1063/1.5005649
50. J.M. de Souza, R.E.B. Ramos Filho, J.B. Duarte, V.M. da Silva, S.R. do Rêgo, L.F.L. de Lucena, W. Acchar, Mechanical and durability properties of compressed stabilized earth brick produced with cassava wastewater. J. Build. Eng. **44**, 103290 (2021). https://doi.org/10.1016/j.jobe.2021.103290
51. H.C. Uzoegbo, Dry-stack and compressed stabilized earth-block construction. In: Nonconventional and vernacular construction materials (Elsevier, 2016), pp. 205–249. https://doi.org/10.1016/B978-0-08-100038-0.00008-1
52. N. Sathiparan, J.H.M. Jaasim, B. Banujan, Sustainable production of cement masonry blocks with the combined use of fly ash and quarry waste. Materialia (Oxf) **26**, 101621 (2022). https://doi.org/10.1016/j.mtla.2022.101621
53. M.S. Shetty, Concrete technology: theory and practice, S. Chand (2005)
54. M. Ahmad, R. Hameed, S. Shahzad, M. Ghous Sohail, Performance evaluation of loadbearing compressed fully recycled aggregate concrete bricks. Structures **55**, 1235–1249 (2023). https://doi.org/10.1016/j.istruc.2023.06.098
55. T. Ali, M.Z. Qureshi, K.C. Onyelowe, E. Althaqafi, A. Deifalla, H. Ahmed, A. Ajwad, Optimizing recycled aggregate concrete performance with chemically and mechanically activated fly ash in combination with coconut fiber. Sci. Rep. **15**(1), 9346 (2025). https://doi.org/10.1038/s41598-025-92227-x
56. E. Hewayde, A. Pachenari, H. Al-Eleaj, Resistance of recycled aggregate concrete (RAC) subjected to drying-wetting cycles to attack of magnesium and sodium sulfates. J. Eng (United Kingdom) **2020**(1), 9746341 (2020). https://doi.org/10.1155/2020/9746341
57. S. Cang, X. Ge, Y. Bao, Assessment of mechanical properties and damage of high performance concrete subjected to magnesium sulfate environment. Adv. Mater. Sci. Eng. **2017**(1), 9196187 (2017). https://doi.org/10.1155/2017/9196187
58. F. Zhang, Z. Hu, F. Wei, X. Wen, X. Li, L. Dai, L. Liu, Study on concrete deterioration in different nacl-na2so4 solutions and the mechanism of cl− diffusion. Materials **14**(17), 5054 (2021). https://doi.org/10.3390/ma14175054
59. F. Zhang, F. Wei, X. Wu, Z. Hu, X. Li, L. Gao, Study on concrete deterioration and chloride ion diffusion mechanism by different

aqueous NaCl-MgSO4 concentrations. Buildings **12**(11), 1843 (2022). https://doi.org/10.3390/buildings12111843
60. Y. Farnam, S. Dick, A. Wiese, J. Davis, D. Bentz, J. Weiss, The influence of calcium chloride deicing salt on phase changes and damage development in cementitious materials. Cem. Concr. Compos. **64**, 1–15 (2015). https://doi.org/10.1016/j.cemconcomp.2015.09.006
61. A.E. Abalaka, Babalaga, Effects of sodium chloride solutions on compressive strength development of concrete containing rice husk ash. ATBU J. Environ. Technol (2011). https://www.journaltocs.ac.uk
62. S.M.S. Kazmi, M.J. Munir, Y.F. Wu, X. Lin, M.R. Ahmad, Investigation of thermal performance of concrete incorporating different types of recycled coarse aggregates. Constr. Build. Mater. **270**, 121433 (2021). https://doi.org/10.1016/j.conbuildmat.2020.121433
63. G.H. Nalon, J.C.L. Ribeiro, L.G. Pedroti, R.M. da Silva, E.N.D. de Araújo, R.F. Santos, G.E.S. de Lima, Review of recent progress on the effects of high temperatures on the mechanical behavior of masonry prisms. Infrastructures (Basel) **8**(7), 112 (2023). https://doi.org/10.3390/infrastructures8070112
64. I. Janotka, T. Nürnbergerová, Effect of temperature on structural quality of the cement paste and high-strength concrete with silica fume. Nucl. Eng. Des. **235**, 2019–2032 (2005). https://doi.org/10.1016/j.nucengdes.2005.05.011
65. K.V. Ramesh, M.D. Raju, K. Rekha, A study on high volume fly ash concrete exposed to elevated temperatures. Am. J. Eng. Res. **5**(11), 227–238 (2016). https://www.ajer.org/papers/v5(11)/ZE05110227238
66. K.P. Mwilongo, R.L. Machunda, Y.A.C. Jande, Effect of elevated temperature on compressive strength and physical properties of neem seed husk ash concrete. Materials **13**, 1198 (2020). https://doi.org/10.3390/ma13051198
67. P. Ren, B. Li, J.G. Yu, T.C. Ling, Utilization of recycled concrete fines and powders to produce alkali-activated slag concrete blocks. J. Clean. Prod. **267**, 122115 (2020). https://doi.org/10.1016/j.jclepro.2020.122115
68. G.B. Bekkeri, K.K. Shetty, G. Nayak, Performance of concrete produced with alkali-activated artificial aggregates. J. Mater. Cycles Waste Manag. **26**, 2024–2042 (2024). https://doi.org/10.1007/s10163-024-01938-2

Publisher's Note Springer Nature remains neutral with regard to jurisdictional claims in published maps and institutional affiliations.